Nanosized ZnO confined inside a Faujasite X zeolite matrix

Bouvy, Claire; Marine, Wladimir; Sporken, Robert; Su, Bao Lian

Published in:
Colloids and surfaces. A: Physicochemical and engineering aspects

DOI:
10.1016/j.colsurfa.2006.12.043

Publication date:
2007

Document Version
Early version, also known as pre-print

Available online at www.sciencedirect.com
ScienceDirect
Colloids and Surfaces A: Physicochem. Eng. Aspects 300 (2007) 145–149
COLLOIDS AND SURFACES A
www.elsevier.com/locate/colsurfa

Nanosized ZnO confined inside a Faujasite X zeolite matrix: Characterization and optical properties

C. Bouvy [a,1], W. Marine [b], R. Sporken [c], B.L. Su [a,*]

[a] *Laboratoire de Chimie des Matériaux Inorganiques (CMI), University of Namur (FUNDP), Rue de Bruxelles 61, B-5000 Namur, Belgium*
[b] *CRMCN, UPR CNRS 7251, Département de Physique, Case 901, Faculté des Sciences de Luminy, Université de la Méditerranée, F-13288 Marseille, Cedex 9, France*
[c] *Laboratoire de Physique des Matériaux Electroniques (LPME), University of Namur (FUNDP), Rue de Bruxelles 61, B-5000 Namur, Belgium*

Received 19 June 2006; received in revised form 15 November 2006; accepted 7 December 2006
Available online 16 December 2006

Abstract

Zinc oxide nanoparticles were introduced inside the porous structure of a Faujasite X zeolite via the impregnation method. N_2 adsorption–desorption analysis, X-ray powder diffraction and photoluminescence spectroscopy were used to characterize the obtained nanocomposites ZnO/FAU. Textural and structural results showed that the presence of ZnO did affect the zeolite structure only when the ZnO precursor solution was quite concentrated. PL results reveal significant blue-shifted emission band which is attributed to quantum size effect (QSE).

Keywords: ZnO; Nanoparticles; Zeolite; Photoluminescence; Quantum size effect

1. Introduction

The preparation of low-dimensional materials, in particular semiconductors, has been largely studied since it is well-known that their optical properties can be tuned by the size of the semiconductor material due to the quantum size effect (QSE) [1,2]. In particular, zinc oxide, a wide band-gap II–VI semiconductor (gap = 3.37 eV, 298 K), shows significant quantum confinement effect (QSE) when its size reaches the Bohr radius, *ca.* 1.8 nm. Moreover, ZnO is an interesting material due to its many applications such as varistors [3,4], gas sensors [5,6], ceramics [7], electrical and optical devices [8,9] and exhibits photoluminescence gain and lasing effect. However, the threshold for lasing was very high [10] and only low-dimensional nanostructures can facilitate lasing.

Both chemical [11–14] and physical [15–17] methods have been employed to synthesize semiconducting nanoparticles but their aggregation remained very often unavoidable. A simply way to solve this problem consists in incorporating nanoparticles inside a porous matrix [18–21] which can limit the particle growth. Zeolitic materials [22,23], in particular Faujasite [24], have been found to be very efficient hosts for the growth of semiconducting nanoparticles due to their small and interconnected porosity. In this study, the Faujasite X zeolite, with 3D channels connected by supercages of 1.3 nm in diameter, has been wetted in $Zn(NO_3)_2$ aqueous solution with different concentrations and the corresponding optical properties were investigated by PL spectroscopy.

2. Experimental

2.1. Nanocomposite preparation

Faujasite X zeolite was synthesized by stirring a sodium aluminate solution with a mixture of NaOH and KOH dissolved in distilled water. After homogenisation, an aqueous sodium silicate solution was rapidly added to the mixture under strong agitation in a molar ratio of $SiO_2/Al_2O_3 = 2.2$. The resulting gel was aged at 70 °C for 24 h before washing and drying. The as-prepared zeolite, labelled here FAU, had a Si/Al ratio of 1 with a chemical composition of $(Na,K)_{96}Si_{96}Al_{96}O_{192}$.

The incorporation of ZnO was performed by impregnation of 0.5 g FAU into 20 ml of a $Zn(NO_3)_2$ aqueous solution with

* Corresponding author. Tel.: +32 81 72 45 31; fax: +32 81 72 54 14.
E-mail address: bao-lian.su@fundp.ac.be (B.L. Su).
[1] FRIA fellow (Fonds National de la Recherche Scienctifique, rue d'Egmont 5, B-1000 Bruxelles, Belgium).

0927-7757/$ – see front matter © 2006 Elsevier B.V. All rights reserved.
doi:10.1016/j.colsurfa.2006.12.043

Table 1
Textural properties of the FAU X zeolite and the ZnO/FAU nanocomposites

	$[Zn(NO_3)_2]$ (M)	ZnO loading (wt.%)	Micropore volume (cm^3/g)	Micropore area (m^2/g)
FAU	0	0	0.30	624
ZnO/FAU-1	0.001	1	0.17	351
ZnO/FAU-2	0.01	4	0.21	424
ZnO/FAU-3	0.05	12	0.18	361
ZnO/FAU-4	0.1	15	0.19	392
ZnO/FAU-5	0.5	19	0.11	221
ZnO/FAU-6	1	14	0.23	464
ZnO/FAU-7	5	44	0.15	314

different concentrations over 20 min. The powder was separated by centrifugation, was dried and calcined under flowing O_2 for 6 h at 550 °C. The obtained powder is labelled ZnO/FAU-X (Table 1). X represents the number of the sample with different ZnO loadings.

2.2. Characterization

Nitrogen adsorption–desorption isotherms were measured at 77 K on a Micromeritics ASAP 2010 instrument. The samples were first degassed under vacuum at 120 °C for several hours. The Horvath–Kawazoe [25] method was used for pore size estimation. The surface areas were determined using the BET equation in the low pressure region ($0.05 \leq p/p_0 \leq 0.25$). X-ray diffraction (XRD) patterns were recorded on a Philips PW1820 diffractometer using Cu Kα radiation with wavelength of 1.54178 Å. PL spectra were recorded at room temperature with an ArF laser (excitation wavelength = 193 nm, pulse duration = 8 ns) as the excitation source and an iCCD camera as the detector. The laser beam was focused onto the sample with a spot size of 2.5×10^{-3} cm^2.

3. Results and discussion

Fig. 1 presents the N_2 adsorption–desorption isotherms of FAU and the FAU/ZnO nanocomposites. Table 1 summarizes these results. The shape of all isotherms (Type I) indicates that the zeolite texture remains intact upon incorporation of ZnO nanoparticles. Moreover, it can be noticed that, at high relative pressure, a hysteresis loop appears due to capillary condensation effect, generally associated with the creation of mesopores [24,26]. However, with increasing the ZnO loadings, the hysteresis loop gradually decreases. This gradual decrease in hysteresis loop is probably due to the location of ZnO particles in mesopores. This suggests that ZnO nanoparticles larger than the size of the supercages can be formed.

Although microporosity is maintained, XRD patterns reveal some changes during the incorporation of ZnO according to the Zn precursor concentration $[Zn(NO_3)_2]$ (Fig. 2). Firstly, a slight shift towards higher 2θ angles is observed for samples ZnO/FAU-5, -6 and -7 (high ZnO loadings). It is noted that the intensity of the first diffraction line (1 1 1) at 6.15° (2θ) and some other diffraction lines such as (2 2 0) at 10.11° (2θ), (3 1 1) at 11.86° (2θ) is sharply increased after incorporation of ZnO

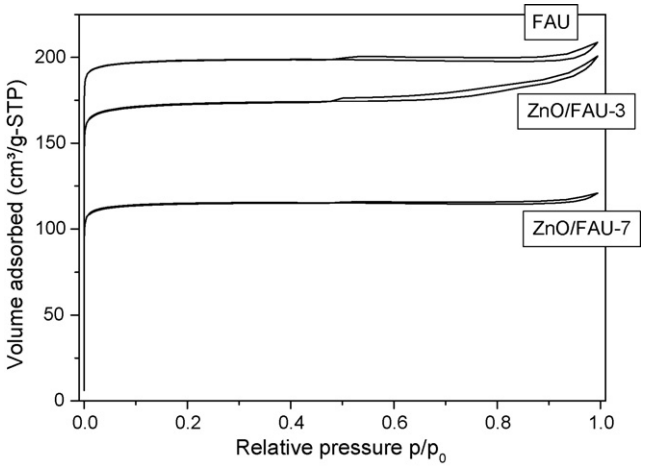

Fig. 1. Nitrogen adsorption–desorption isotherms of (a) Faujasite X matrix, ZnO/FAU-1, -4 and -7 and (b) correlation between the surface area and the concentration of the $Zn(NO_3)_2$ solution.

nanoparticles. This increase in intensity of the first diffraction line is often observed in Na form Faujasite zeolites after ion exchange with bivalent cations like Ca^{2+} since the introduction of bivalent Ca^{2+} ions to replace monovalent Na^+ ions (one Ca^{2+} for Na^+ ions) will change the symmetry of crystalline structure from *Fd*3 (Na-FAU) to *Fd*3*m* (NaCa-FAU) [27]. This indicates that the formation of ZnO nanoparticles in Faujasite zeolite will change the symmetry of the system. It is also possible that ion exchange can occur and some Zn^{2+} ions replace Na^+ ions to play the role of the compensating ions. Moreover, no diffraction peaks of bulk ZnO could be observed except for sample ZnO/FAU-7 which is the most loaded nanocomposite (ZnO diffraction peaks marked with a star *). For this latter case, it is believed that ZnO particles have grown on the external surface of the zeolite matrix. For the other samples, the ZnO nanoparticles are included inside

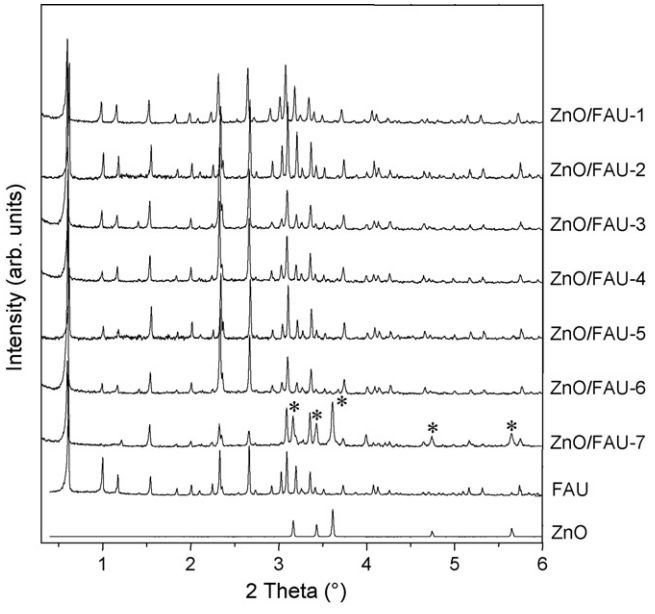

Fig. 2. Powder XRD patterns of (a) Faujasite X zeolite matrix and (b) ZnO-FAU.

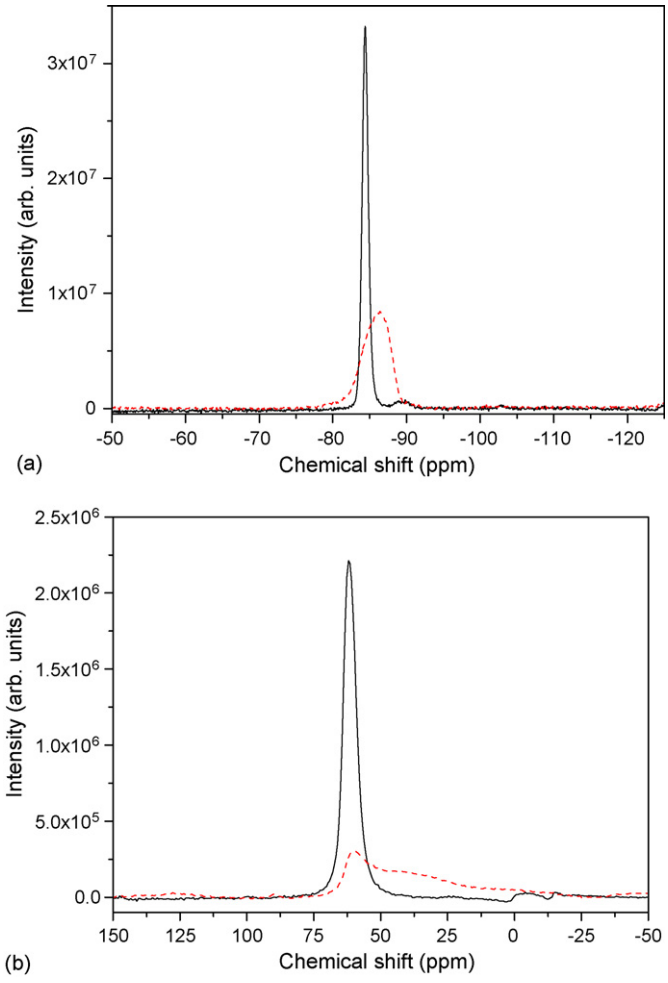

Fig. 3. (a) NMR ^{29}Si spectra of FAU (solid line) and ZnO/FAU-6 (dashed line) and (b) NMR ^{27}Al spectra of FAU (solid line) and ZnO/FAU-6 (dashed line).

the channels of the zeolite and are too small to give the corresponding diffraction pattern. This has already been observed by different authors in several cases [28–30].

In order to gain a deeper understanding of the structural changes observed within the Faujasite crystallites after the incorporation of ZnO, ^{29}Si and ^{27}Al NMR were performed on a representative sample, ZnO/FAU-6 (Fig. 3 and Table 2).

For the ^{29}Si NMR spectra the signal at −84 ppm was assigned to Si atoms with 4 Al neighbours while for the ^{27}Al NMR spectra, the resonance centred around 60 ppm represents tetrahedrally coordinated Al. In both cases, except for the small shift of the signal position, an important broadening of the bands is observed. This broadening can be explained by the interaction created

Table 2
Chemical shifts and widths of the NMR bands of FAU X zeolite and ZnO-FAU-6 nanocomposite

	^{29}Si (ppm)		^{27}Al (ppm)	
	Chemical shift	FWHM	Chemical shift	FWHM
FAU	−84	0.95	63	5.5
ZnO/FAU-6	−86	4.5	60 (+39)	7.5

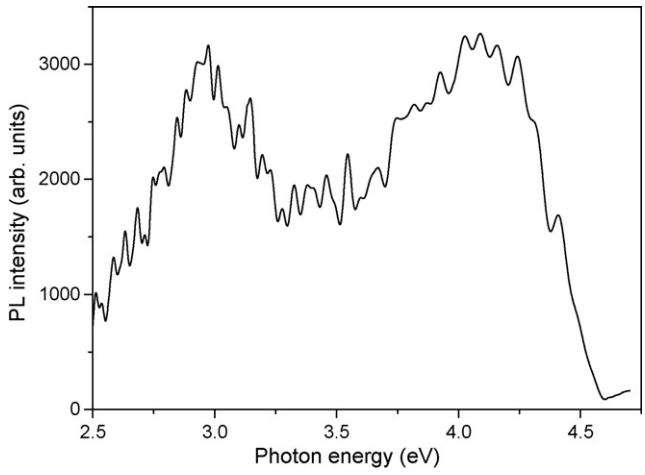

Fig. 4. PL spectra of the Faujasite X zeolite (E_{exc} = 6.4 eV).

between the ZnO nanoparticles and the FAU internal surface and also by the symmetrical changes observed in the XRD patterns. These observations led to a preliminary conclusion that during the growth of ZnO nanoparticles inside the Faujasite, textural properties were conserved and that some symmetrical changes did occur but without the collapse of the zeolite framework. From this, it can be affirmed that the growth of the nanoparticles has been well limited by the zeolite walls.

At low $Zn(NO_3)_2$ concentrations, no significant shift in the XRD patterns could be observed. As it will be seen in PL spectra, when the ZnO precursor concentration is too low, Zn ions simply take place in the channels of the Faujasite zeolite and an ion exchange can occur to replace Na^+ and K^+ ions. Thus, upon calcination under O_2, no ZnO particles can be formed. When the $Zn(NO_3)_2$ solution becomes more concentrated, more Zn ions can enter the zeolite and, in addition to ion exchange process, ZnO particles can really be formed after the calcination under O_2. Therefore, the structure can be affected by the presence of ZnO and a shift in the XRD patterns is observed.

Photoluminescence spectroscopy measurements were performed at room temperature using an ArF laser (6.4 eV) as excitation source. In order to understand how the PL properties evolve with the ZnO loading, the PL spectrum of the Faujasite X zeolite matrix is presented in Fig. 4. Two broad bands are observed at 3.0 and 4.0 eV. This weak photoluminescence is still undetermined owing to an absence of information on the optical properties of zeolites within the literature.

The corresponding PL spectra of ZnO/FAU are shown in Fig. 5(a) and (b). At low $Zn(NO_3)_2$ concentrations (samples ZnO/FAU-1, -2 and -3, Fig. 4(a)), the same two weak and broad bands are observed, confirming the absence of ZnO particles in spite of the presence of Zn^{2+} ions as counter-ions inside the zeolite. At this stage, as already said, the Zn ions enter the structure but do not form ZnO particles after calcination. The PL intensities of the spectra are slightly higher suggesting that some defects of the zeolite matrix, which can give rise to PL bands, are passivated by the presence of Zn ions. At high $Zn(NO_3)_2$ concentrations (samples ZnO/FAU-4, -5, -6 and -

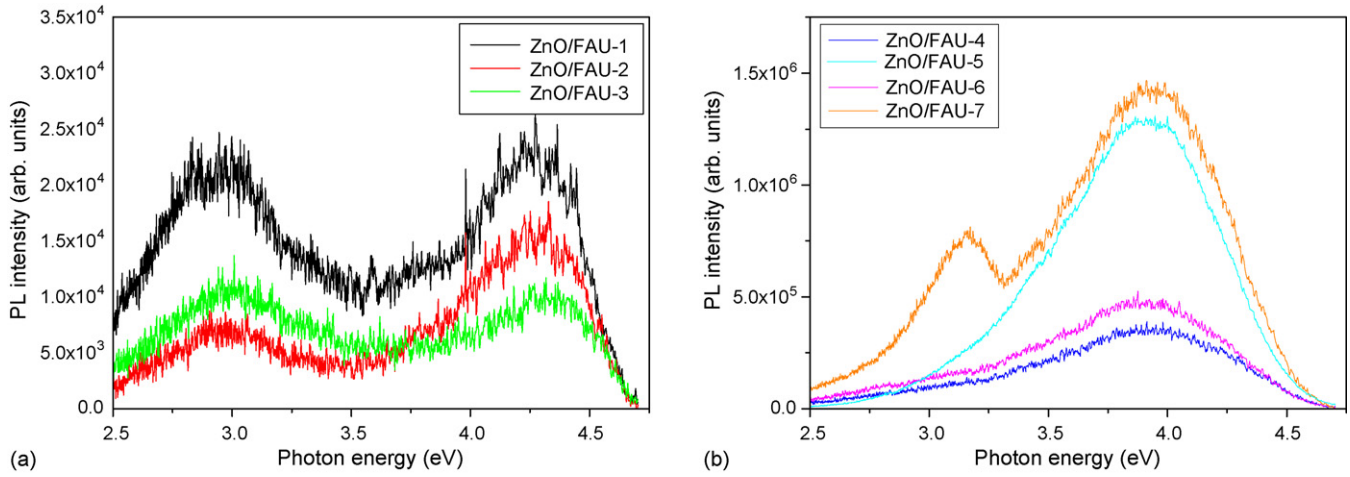

Fig. 5. PL spectra of the ZnO/FAU-1, -2 and -3 nanocomposites (a) and the ZnO-FAU-4, -5, -6 and -7 nanocomposite (b) (E_{exc} = 6.4 eV).

7, Fig. 4(b)), only one broad and very intense band centred at 3.9 eV is observed in PL spectra, meaning that ZnO particles are really formed. The PL band of bulk ZnO is usually observed at 3.3 eV. The shift towards higher energies is attributed to quantum size effect arising from very small ZnO nanoparticles confined inside the channels and supercages of the Faujasite zeolite matrix.

It has to note that, for sample ZnO/FAU-7, a second band is observed at 3.2 eV. It has already been seen that ZnO diffraction peaks were present in the XRD pattern of this sample. We can thus conclude that, in this case, bigger ZnO particles were formed probably, outside the zeolite network.

4. Conclusions

The Faujasite X zeolite has been chosen as host for the incorporation of ZnO nanoparticles because of its 3D channels and supercages which allow to limit the particle size of ZnO during the growth. The particles were loaded inside the network of the matrix via the impregnation method which implies the suspension of the zeolite in various $Zn(NO_3)_2$ aqueous solution followed by calcination under flowing O_2. N_2 adsorption–desorption analysis provides evidences of the ZnO incorporation inside the structure. XRD patterns reveal that the structure was affected only when the ZnO precursor concentration was important. The PL study indicates that, when the ZnO precursor concentration was quite low, no emission band of ZnO could be observed. Otherwise, when the concentration increased, a blue-shifted emission band was clearly visible and was attributed to quantum size effect of ZnO nanoparticles formed inside the Faujasite X matrix.

Acknowledgments

C. Bouvy thanks the FRIA (Fonds National de la Recherche Scientifique, Belgium) for a doctoral fellowship. Financial supports from the University of Namur (FUNDP) and from the European SOXESS network are gratefully acknowledged.

References

[1] L.E. Brus, J. Chem. Phys. 80 (1984) 4403–4409.
[2] A. Henglein, Chem. Rev. 89 (1989) 1861–1873.
[3] D.R. Clarke, J. Am. Ceram. Soc. 82 (1999) 485–502.
[4] N.T. Hung, N.D. Quang, S. Bernik, J. Mater. Res. 16 (2001) 2817–2823.
[5] Y. Shimizu, F.C. Lin, Y. Takao, M. Egashira, J. Am. Ceram. Soc. 81 (1998) 1633–1643.
[6] R. Paneva, D. Gotchev, Sens. Actuators A: Phys. 72 (1999) 79–87.
[7] L. Gao, Q. Li, W.L. Luan, J. Am. Ceram. Soc. 85 (2002) 1016–1018.
[8] B.D. Yao, H.Z. Shi, H.J. Bi, L.D. Zhang, J. Phys. Condensed Matter 12 (2000) 6265–6270.
[9] Y.C. Kong, D.P. Yu, B. Zhang, W. Fang, S.Q. Feng, Appl. Phys. Lett. 78 (2001) 407–409.
[10] J.C. Johnson, H. Yan, R.D. Schaller, L.H. Haber, R.J. Saykally, P. Yang, J. Phys. Chem. B 105 (2001) 11387–11390.
[11] R. Reisfeld, J. Alloys Compd. 341 (2002) 56–61.
[12] C. Cannas, C. Casu, A. Musinu, A. Lai, G. Piccaluga, J. Mater. Chem. 9 (1999) 1765–1769.
[13] S. Music, D. Dragcevic, S. Popovic, M. Ivanda, Mater. Lett. 59 (2005) 2388–2393.
[14] U. Koch, A. Fojtik, H. Weller, A. Henglein, Chem. Phys. Lett. 122 (1985) 507–510.
[15] I. Ozerov, D. Nelson, A.V. Bulgakov, W. Marine, M. Sentis, Appl. Surf. Sci. 212/213 (2003) 349–352.
[16] C. Munuera, J. Zuniga-Perez, J.F. Rommeluere, V. Sallet, R. Triboulet, F. Soria, V. Munoz-Sanjose, C. Ocal, J. Cryst. Growth 264 (2004) 70–78.
[17] D.M. Bagnall, Y.F. Chen, Z. Zhu, T. Yao, S. Koyama, M.Y. Shen, T. Goto, Appl. Phys. Lett. 70 (1997) 2230–2232.
[18] W.H. Zhang, J.L. Shi, L.Z. Wang, D.S. Yan, Chem. Mater. 12 (2000) 1408–1413.
[19] S.E. Dapurkar, S.K. Badamali, P. Selvam, Catal. Today 68 (2001) 63–68.
[20] E. Dalas, J. Kallitsis, S. Sakkopoulos, E. Vitoratos, P.G. Koutsoukos, J. Colloid Interf. Sci. 141 (1991) 137–145.
[21] M. Oner, J. Norwig, W.H. Meyer, G. Wegner, Chem. Mater. 10 (1998) 460–463.
[22] H. Villavicencio-Garcia, M. Hernandez-Velez, O. Sanchez-Garrido, J.M. Martinez-Duart, J. Jimenez, Solid State Electron. 43 (1999) 1171–1175.
[23] R.J. Martin-Palma, M. Hernandez-Velez, I. Diaz, H. Villavicencio-Garcia, M.M. Garcia-Poza, J.M. Martinez-Duart, J. Perez-Pariente, Mater. Sci. Eng. C 15 (2001) 163–166.

[24] M. Wark, H. Kessler, G. Schulz-Ekloff, Microporous Mater. 8 (1997) 241–253.
[25] G. Hortvath, K.J. Kawazoe, J. Chem. Eng. Jpn. 16 (1983) 470–475.
[26] J. Rathousky, A. Zukal, N. Jaeger, G. Sschulz-Ekloff, J. Chem. Soc., Faraday Trans. 88 (1992) 489–495.
[27] M.M.J. Treacy, J.B. Higgins, Collections of Simulated XRD Powder Patterns for Zeolites, Elsevier, Amsterdam, 2001.
[28] F. Meneau, G. Sankar, N. Morgante, S. Cristol, C.R.A. Catlow, J.M. Thomas, G.N. Greaves, Nucl. Instrum. Methods Phys. Res. B 199 (2003) 499–503.
[29] F. Iacomi, Formation of semiconductor clusters in zeolites, Surf. Sci. 532–535 (2003) 816–821.
[30] J. Chen, Z. Feng, P. Ying, C. Li, J. Phys. Chem. B 108 (2004) 12669–12676.